EUROPEAN JOURNAL OF PURE AND APPLIED MATHEMATICS
2025, Vol. 18, Issue 4, Article Number 6776
ISSN 1307-5543 – ejpam.com
Published by New York Business Global

Stochastic Dynamics of Epidemic Models with Resource Constraints: Extinction and Ergodicity

J. Leo Amalraj[1], Manivannan Balamurugan[2], Pankaj Shukla[3], M. V. Rajesh[4], N. Avinash[5], Vediyappan Govindan[6], Siriluk Donganont[7,*]

[1] *Department of Mathematics, RMK College of Engineering and Technology, Puduvoyal, Thiruvallur, Tamil Nadu, India*
[2] *Department of Mathematics, Vel Tech Rangarajan Dr. Sagunthala R&D Institute of Science and Technology, Chennai 600 062, Tamil Nadu, India*
[3] *Department of Mathematics, School of Advanced Sciences, Vellore Institute of Technology, Chennai, Tamil Nadu, India*
[4] *Department of Information Technology, Aditya University, Surampalem, India*
[5] *Department of Mathematics, Sacred Heart College (Autonomous), Tirupattur 635 601, Tamil Nadu, India*
[6] *Department of Mathematics, Hindustan Institute of Technology and Science, Chennai, Tamil Nadu, India*
[7] *School of Science, University of Phayao, Phayao 56000, Thailand*

Abstract. Recent studies highlight how stochastic effects, such as environmental noise and resource constraints, alter epidemic dynamics, diverging from deterministic predictions. Unlike classical deterministic models that exhibit backward and Hopf bifurcations, stochastic models incorporating white noise perturbations capture more realistic outbreak scenarios by smoothing transitions and expanding extinction regions. This paper analyzes a stochastic SIR model with nonlinear incidence $\frac{\beta SI}{1+kI}$, limited medical resources modeled as $\frac{\alpha I}{\lambda+I}$, and environmental noise via Brownian motion terms. Research suggests that limited medical resources, coupled with stochastic fluctuations, significantly influence disease spread, persistence, and extinction conditions, as governed by a stochastic threshold η. Numerical simulations, including bifurcation surfaces and trajectory comparisons, support these findings, demonstrating how noise eliminates bifurcations and promotes disease control. These insights emphasize the need for randomness in epidemic modeling to improve predictive accuracy and inform public health interventions. Understanding these stochastic influences can aid in developing more adaptive policies for epidemic mitigation, particularly in resource-limited settings. Future research aims to refine these models by incorporating spatial heterogeneity, population diversity, time delays, and pathogen evolution for better epidemic control.

2020 Mathematics Subject Classifications: 92D30, 60J28, 34F10, 92C60, 37N25

Key Words and Phrases: Stochastic modeling, SIR model, backward bifurcation, medical resources, disease dynamics

*Corresponding author.
DOI: https://doi.org/10.29020/nybg.ejpam.v18i4.6776

Email addresses: leoamalraj@rmkcet.ac.in (J. Leo Amalraj), balamurugansvm@gmail.com (M. Balamurugan), pankaj.shukla@vit.ac.in (P. Shukla), rajesh.masina@adityauniversity.in (M. V. Rajesh), avinashprofess@gmail.com (N. Avinash), vgovindandr@gmail.com (V. Govindan), siriluk.pa@up.ac.th (S. Donganont)

1. Introduction

Infectious diseases, such as tuberculosis (TB), HIV, and emerging threats like COVID-19, continue to impose a substantial global health burden. Rapid urbanization, climate change, and increasing human aggregation exacerbate the spread of these diseases, necessitating advanced tools for prediction and control. Tuberculosis, caused by *Mycobacterium tuberculosis*, remains a leading cause of mortality, claiming 1.18 million lives in 2017, while HIV-related illnesses accounted for 940,000 deaths in the same year [1]. The COVID-19 pandemic, with over 21 million cases by August 2020, underscores the urgency of addressing these challenges [1]. Cutting-edge epidemic modeling, particularly approaches incorporating stochasticity and resource constraints, offers critical insights into disease dynamics, enabling more effective public health strategies [2].

Stochastic modeling is a cornerstone for analyzing complex systems influenced by randomness, with applications spanning biology, finance, engineering, and physics [3]. By leveraging probability theory, statistical inference, and techniques like Markov chains, Brownian motion, and Monte Carlo simulations, these models quantify uncertainty and identify key drivers in dynamic systems. In epidemiology, stochastic models enhance the understanding of irregular epidemic patterns, such as those observed in COVID-19, by accounting for demographic noise and environmental disturbances [4]. For instance, research on susceptible–infected–recovered (SIR) models reveals that stochastic noise expands Turing instability regions, leading to unpredictable disease spread [4]. Similarly, susceptible–vaccinated–infected–recovered (SVIR) models explore dual-disease dynamics and vaccination strategies, using Lyapunov functions and numerical methods like the Milstein scheme to assess disease extinction conditions [5]. Unlike deterministic models, which assume constant parameters, stochastic approaches capture real-world variability, making them indispensable for realistic epidemic predictions [6–10]. Recent advancements in stochastic epidemic modeling include multiphasic models for phased outbreaks [11], SEIQR models with generalized incidence and environmental noise [12], and SIR variants incorporating Ornstein-Uhlenbeck processes for individual heterogeneity [13], as well as models with telegraph and Lévy noise for abrupt environmental changes [14].

Industrial progress has improved living standards but introduced significant environmental challenges, notably air pollution from coal-based energy sources emitting pollutants like SO_2, NO, O_3, CO, and particulate matter (PM) [15]. Fine particles (PM2.5) pose severe risks, penetrating deep into the lungs and bloodstream, contributing to respiratory and cardiovascular diseases such as asthma, chronic obstructive pulmonary disease (COPD), and heart disease [16]. The Air Quality Index (AQI), a standardized tool, communicates pollution severity and health risks, guiding public health responses [15]. However, research on ultrafine particles (UFP) remains limited, with only one large-scale study examining long-term exposure [17–19]. Standardized monitoring for UFPs could unlock new insights into their health impacts, addressing a critical gap in environmental health research.

Epidemic models are vital for informing public health strategies, yet traditional approaches often overlook stochastic factors like white noise, telegraph noise, and Lévy noise,

which significantly influence disease persistence and extinction [6]. Recent studies integrating these elements have improved prediction accuracy, particularly for abrupt environmental changes [6]. Markov chain processes and regime-switching models, such as stochastic SIS models, further enhance realism by accounting for environmental fluctuations like weather or food supply changes [7–10]. The COVID-19 pandemic highlighted the importance of such models, with adaptations incorporating fractional-order equations and fuzzy Caputo methods to capture complex dynamics [7–10].

Intervention strategies, both pharmaceutical (e.g., vaccination) and non-pharmaceutical (e.g., social distancing, mask-wearing), are critical for controlling disease spread [20, 21]. Behavioral responses, such as condom use for STI prevention or mask adherence during COVID-19, shape epidemic trajectories and must be integrated into models for effective control [20, 21]. Zoonotic diseases like SARS-CoV-2, which lack preexisting immunity, underscore the reliance on early non-pharmaceutical interventions, despite their social and economic costs [22–24]. Policymakers have leaned on epidemic models to navigate these trade-offs, though comparing predictions remains challenging without robust numerical and theoretical frameworks [22–24].

The rise of emerging infectious diseases (EIDs) like COVID-19 emphasizes the need to understand immune responses and transmission dynamics [25]. Research on backward bifurcation and immunity decline reveals complex patterns, highlighting the role of mathematical modeling in crafting control strategies [25]. By May 2020, COVID-19 had caused over 6.2 million cases and 372,344 deaths globally, yet national response strategies prevented hundreds of thousands of cases in several countries [26, 27]. The World Health Organization's six criteria for lifting lockdowns—controlled transmission, healthcare readiness, and community engagement—underscore the need for strategic planning to prevent resurgence [28, 29]. Tools like SWOT analysis have further supported pandemic control by fostering resource integration across sectors [26, 27].

Tuberculosis remains a global health priority, primarily transmitted through airborne droplets and influenced by factors like exposure duration and environmental conditions [30, 31]. While the immune system often controls TB bacteria, unchecked proliferation leads to active disease, posing significant public health risks in high-prevalence regions [31, 32]. Similarly, pneumonia, driven by pathogens like *Streptococcus pneumoniae*, is a leading cause of morbidity and mortality, particularly among vulnerable populations [33]. Vaccines like PCV and PPV offer preventive benefits, but comprehensive strategies combining immunization, treatment, and environmental controls are essential for eradication [33].

Beyond modeling and interventions, systemic improvements in healthcare are crucial for addressing infectious diseases. While simulation-based training enhances patient safety, it must be paired with structural changes, cultural shifts, and process improvements to ensure lasting impact [34]. These efforts, combined with advanced modeling and environmental monitoring, form a holistic approach to tackling global health challenges.

The interplay of infectious diseases, environmental factors, and stochastic dynamics demands innovative solutions. Stochastic modeling, with its ability to capture uncertainty and variability, offers a powerful tool for predicting and controlling epidemics.

Coupled with robust intervention strategies and systemic healthcare improvements, these approaches can mitigate the global burden of diseases like TB, HIV, and COVID-19. Continued research into environmental health, particularly air pollution and UFPs, will further strengthen public health responses, paving the way for a more resilient future.

2. Long-Term Behavior of the Epidemic

We investigate the persistence of an infectious disease using a stochastic model, focusing on the susceptible ($\mathcal{S}(t)$) and infected ($\mathcal{I}(t)$) populations. Define the positive cone:

$$\mathbb{R}^2_+ = \{(x, y) \in \mathbb{R}^2 : x > 0, y > 0\},$$

representing biologically relevant states.

Here, $\mathcal{S}(t)$ (or simply $S(t)$) represents the number of susceptible individuals in the population at time t.

Lemma 1. *For any initial condition $(\mathcal{S}(0), \mathcal{I}(0)) \in \mathbb{R}^2_+$, the solution to the stochastic system:*

$$\begin{cases} d\mathcal{S}(t) = \left(\Lambda - \frac{\beta \mathcal{S}(t)\mathcal{I}(t)}{1+k\mathcal{I}(t)} - \delta \mathcal{S}(t)\right) dt - \frac{\sigma \mathcal{S}(t)\mathcal{I}(t)}{1+k\mathcal{I}(t)} dB(t), \\ d\mathcal{I}(t) = \left(\frac{\beta \mathcal{S}(t)\mathcal{I}(t)}{1+k\mathcal{I}(t)} - (\delta + \gamma + \epsilon)\mathcal{I}(t) - \frac{\alpha \mathcal{I}(t)}{\lambda + \mathcal{I}(t)}\right) dt + \frac{\sigma \mathcal{S}(t)\mathcal{I}(t)}{1+k\mathcal{I}(t)} dB(t), \end{cases} \tag{1}$$

remains in $\mathbb{R}^2_+$ for all $t \geq 0$ almost surely, i.e., $\mathbb{P}((\mathcal{S}(t), \mathcal{I}(t)) \in \mathbb{R}^2_+ \ \forall t \geq 0) = 1$.

Proof. The system (1) has locally Lipschitz coefficients, ensuring a unique solution up to an explosion time $\tau^* \in (0, \infty]$. Solving explicitly, we obtain:

$$\mathcal{S}(t) = \mathcal{S}(0) \exp\left(\int_0^t \left(-\frac{\beta \mathcal{I}(u)}{1 + k\mathcal{I}(u)} - \delta - \frac{\sigma^2 \mathcal{I}^2(u)}{2(1 + k\mathcal{I}(u))^2}\right) du - \int_0^t \frac{\sigma \mathcal{I}(u)}{1 + k\mathcal{I}(u)} dB(u)\right),$$

$$\mathcal{I}(t) = \mathcal{I}(0) \exp\left(\int_0^t \left(\frac{\beta \mathcal{S}(u)}{1 + k\mathcal{I}(u)} - (\delta + \gamma + \epsilon) - \frac{\alpha}{\lambda + \mathcal{I}(u)} - \frac{\sigma^2 \mathcal{S}^2(u)}{2(1 + k\mathcal{I}(u))^2}\right) du + \int_0^t \frac{\sigma \mathcal{S}(u)}{1 + k\mathcal{I}(u)} dB(u)\right).$$

Since $\mathcal{S}(0), \mathcal{I}(0) > 0$, the exponential terms guarantee positivity for $t < \tau^*$.

To prove $\tau^* = \infty$ almost surely, suppose $\mathbb{P}(\tau^* < \infty) > 0$. Then, there exist $T, \kappa > 0$ such that $\mathbb{P}(\tau^* < T) > \kappa$. Define the stopping time:

$$\tau_n = \inf\{t \in (0, \tau^*) : \mathcal{S}(t) + \mathcal{I}(t) \geq n\}.$$

For large n, $\mathbb{P}(\tau_n < T) > \kappa$. Summing (1):

$$d(\mathcal{S} + \mathcal{I}) \leq (\Lambda - \delta(\mathcal{S} + \mathcal{I}))\, dt,$$

since $(\gamma + \epsilon)\mathcal{I} + \frac{\alpha \mathcal{I}}{\lambda + \mathcal{I}} \geq 0$. Integrating over $[0, t \wedge \tau_n]$:

$$\mathcal{S}(t \wedge \tau_n) + \mathcal{I}(t \wedge \tau_n) \leq \mathcal{S}(0) + \mathcal{I}(0) + \Lambda(t \wedge \tau_n).$$

Taking expectations:

$$\mathbb{E}[\mathcal{S}(\tau_n) + \mathcal{I}(\tau_n)] \leq \mathcal{S}(0) + \mathcal{I}(0) + \Lambda T.$$

Since $\mathcal{S}(\tau_n) + \mathcal{I}(\tau_n) \geq n$ on $\{\tau_n < T\}$, we get $n\kappa \leq \mathcal{S}(0) + \mathcal{I}(0) + \Lambda T$, a contradiction as $n \to \infty$. Thus, $\mathbb{P}(\tau^* < \infty) = 0$, ensuring positivity.

To ensure the model's biological realism, we confirm that solutions remain bounded within an invariant region.

Lemma 2. *Define the region:*

$$\mathcal{D} = \left\{(x, y) \in \mathbb{R}^2_+ : z^* < x + y < \frac{\Lambda}{\delta}\right\},$$

where z^* is the unique root of:

$$\psi(z) = \Lambda - (\delta + \gamma + \epsilon)z - \frac{\alpha z}{\lambda + z}. \tag{2}$$

Then, $\mathcal{D}$ is positively invariant and attractive for (1).

Proof. Let $\mathcal{Z}(t) = \mathcal{S}(t) + \mathcal{I}(t)$. From (1):

$$\frac{d\mathcal{Z}}{dt} = \Lambda - \delta\mathcal{Z} - (\gamma + \epsilon)\mathcal{I} - \frac{\alpha\mathcal{I}}{\lambda + \mathcal{I}}.$$

Since $\mathcal{I} \leq \mathcal{Z}$:

$$\frac{d\mathcal{Z}}{dt} \leq \Lambda - \delta\mathcal{Z}.$$

Consider the comparison equation:

$$\frac{d\bar{\mathcal{Z}}}{dt} = \Lambda - \delta\bar{\mathcal{Z}}, \quad \bar{\mathcal{Z}}(0) = \mathcal{Z}(0).$$

Solving:

$$\bar{\mathcal{Z}}(t) = \frac{\Lambda}{\delta} + \left(\mathcal{Z}(0) - \frac{\Lambda}{\delta}\right) e^{-\delta t}.$$

Thus, $\lim_{t\to\infty} \bar{\mathcal{Z}}(t) = \frac{\Lambda}{\delta}$, and $\mathcal{Z}(t) \leq \bar{\mathcal{Z}}(t)$. Now:

$$\frac{d\mathcal{Z}}{dt} \geq \psi(\mathcal{Z}),$$

where $\psi(z)$ is decreasing, with $\psi(0) = \Lambda > 0$, $\psi(\Lambda/\delta) < 0$. Hence, $\psi(z^*) = 0$ for a unique $z^* \in (0, \Lambda/\delta)$. By comparison, if $\mathcal{Z}(0) > z^*$, then $\mathcal{Z}(t) \geq z^*$.

For attractivity, if $\mathcal{Z}(0) > \Lambda/\delta$:

$$\frac{d\mathcal{Z}}{dt}\Big|_{\mathcal{Z}=\Lambda/\delta+a} < -\delta a,$$

so $\mathcal{Z}(t)$ decreases toward Λ/δ. If $\mathcal{Z}(0) < z^*$, then $\psi(\mathcal{Z}) > 0$, so $\mathcal{Z}(t)$ increases toward z^*. Thus, $\mathcal{D}$ is invariant and attractive.

We now analyze the persistence of the infected population within $\mathcal{D}$.

Theorem 1. *For $(\mathcal{S}(0), \mathcal{I}(0)) \in \mathcal{D}$, the disease goes extinct if:*

$$\eta = \frac{\beta\Lambda}{\delta} - (\delta + \gamma + \epsilon) - \frac{\alpha}{\lambda} - \frac{1}{2}\sigma^2 \left(\frac{\Lambda}{\delta}\right)^2 < 0. \tag{3}$$

then:

$$\liminf_{t\to\infty} \mathbb{E}[\mathcal{I}(t)] \geq m_I,$$

where $m_I > 0$ is a constant.

Proof. Define:

$$\xi = \frac{\beta\Lambda}{\delta} - \left(\delta + \gamma + \epsilon + \frac{\alpha}{\lambda} + \frac{\sigma^2\Lambda^2}{2\delta^2}\right).$$

By (3), $\xi > 0$. Consider the Lyapunov function:

$$W(\mathcal{S}, \mathcal{I}) = \left(1 + \frac{\Lambda}{\delta} - \mathcal{S}\right)\mathcal{I}^{-\theta},$$

where $\theta > 0$ satisfies:

$$\theta < \frac{2\xi}{\sigma^2}.$$

By Itô's lemma:

$$dW = \mathcal{L}W dt + \frac{\sigma\mathcal{S}\mathcal{I}^{-\theta}}{1 + k\mathcal{I}}\left[\mathcal{I} - \theta\left(1 + \frac{\Lambda}{\delta} - \mathcal{S}\right)\right] dB(t),$$

where:

$$\mathcal{L}W = \left(\Lambda - \frac{\beta\mathcal{S}\mathcal{I}}{1 + k\mathcal{I}} - \delta\mathcal{S}\right)\mathcal{I}^{-\theta} - \theta\left(1 + \frac{\Lambda}{\delta} - \mathcal{S}\right)\mathcal{I}^{-\theta}\left(\frac{\beta\mathcal{S}}{1 + k\mathcal{I}} - (\delta + \gamma + \epsilon) - \frac{\alpha}{\lambda + \mathcal{I}} + \frac{\sigma^2\mathcal{S}^2(1 + \theta)}{2(1 + k\mathcal{I})^2}\right).$$

Bounding $\mathcal{L}W$:

$$\mathcal{L}W \leq \kappa_1 - \kappa_2 W,$$

with:

$$\kappa_1 = \Lambda\left(\frac{\Lambda}{\delta}\right)^{-\theta}, \quad \kappa_2 = \theta\xi.$$

Applying Itô's lemma to $e^{\kappa_2 t}W$ and taking expectations:

$$\mathbb{E}[e^{\kappa_2 t}W(t)] \leq W(0) + \frac{\kappa_1}{\kappa_2}(e^{\kappa_2 t} - 1).$$

Thus:

$$\mathbb{E}[\mathcal{I}^{-\theta}(t)] \leq \frac{W(0)e^{-\kappa_2 t} + \frac{\kappa_1}{\kappa_2}(1 - e^{-\kappa_2 t})}{1 + \frac{\Lambda}{\delta}}.$$

By Jensen's inequality:

$$\mathbb{E}[\mathcal{I}(t)] \geq \left(\frac{\kappa_1}{\kappa_2}\right)^{-1/\theta} \text{ as } t \to \infty.$$

Hence, $\liminf_{t\to\infty} \mathbb{E}[\mathcal{I}(t)] \geq m_I = \left(\frac{\kappa_1}{\kappa_2}\right)^{-1/\theta}$.

Proposition 1. *For any initial condition* $(\mathcal{S}(0), \mathcal{I}(0)) \in \mathcal{D}$,

$$\liminf_{t\to\infty} \mathbb{E}[\mathcal{S}(t)] \geq \frac{\Lambda}{\delta + \beta\frac{\Lambda}{\delta}}.$$

This provides a lower bound on the expected susceptible population, assuming the infected population is bounded above by $\frac{\Lambda}{\delta}$.

Proof. From (1),

$$\frac{d}{dt}\mathbb{E}[\mathcal{S}(t)] = \mathbb{E}\left[\Lambda - \frac{\beta\mathcal{S}(t)\mathcal{I}(t)}{1+k\mathcal{I}(t)} - \delta\mathcal{S}(t)\right].$$

Since $\mathcal{I}(t) \leq \frac{\Lambda}{\delta}$ and $\frac{\mathcal{I}(t)}{1+k\mathcal{I}(t)} \leq \frac{\mathcal{I}(t)}{k\mathcal{I}(t)} = \frac{1}{k}$ for large $\mathcal{I}$, but more tightly, $\frac{\beta\mathcal{S}\mathcal{I}}{1+k\mathcal{I}} \leq \beta\mathcal{S}\mathcal{I} \leq \beta\mathcal{S}\frac{\Lambda}{\delta}$,

$$\frac{d}{dt}\mathbb{E}[\mathcal{S}(t)] \geq \Lambda - \delta\mathbb{E}[\mathcal{S}(t)] - \beta\frac{\Lambda}{\delta}\mathbb{E}[\mathcal{S}(t)].$$

Solving the comparison ODE yields the bound as $t \to \infty$.

Proposition 2. *For* $(\mathcal{S}(0), \mathcal{I}(0)) \in \mathcal{D}$*:*

$$\limsup_{t\to\infty} \mathbb{E}[\mathcal{S}^{-1}(t)] \leq \frac{\delta + \frac{\beta\Lambda}{\delta} + \frac{\sigma^2\Lambda^2}{\delta^2}}{\Lambda}.$$

Proof. Apply Itô's lemma to $\mathcal{S}^{-1}$:

$$d(\mathcal{S}^{-1}) = \left(-\Lambda\mathcal{S}^{-2} + \frac{\beta\mathcal{I}\mathcal{S}^{-1}}{1+k\mathcal{I}} + \delta\mathcal{S}^{-1} + \frac{\sigma^2\mathcal{I}^2\mathcal{S}^{-1}}{(1+k\mathcal{I})^2}\right)dt + \frac{\sigma\mathcal{I}\mathcal{S}^{-1}}{1+k\mathcal{I}}dB(t).$$

Since $\mathcal{I} \leq \frac{\Lambda}{\delta}$:

$$\frac{\beta\mathcal{I}}{1+k\mathcal{I}} + \frac{\sigma^2\mathcal{I}^2}{(1+k\mathcal{I})^2} \leq \frac{\beta\Lambda}{\delta} + \frac{\sigma^2\Lambda^2}{\delta^2}.$$

Thus:

$$d(\mathcal{S}^{-1}) \leq \left(-\Lambda\mathcal{S}^{-2} + \left(\delta + \frac{\beta\Lambda}{\delta} + \frac{\sigma^2\Lambda^2}{\delta^2}\right)\mathcal{S}^{-1}\right)dt + \text{stochastic term}.$$

Using the inequality $-\Lambda x^{-2} + ax^{-1} \leq \frac{a^2}{4\Lambda}$ (derived by completing the square: let $f(x) = -\Lambda x^{-2} + ax^{-1}$, maximum at $x^{-1} = \frac{a}{2\Lambda}$, yielding $\frac{a^2}{4\Lambda}$),

$$\frac{d}{dt}\mathbb{E}[\mathcal{S}^{-1}] \leq \frac{\left(\delta + \beta\frac{\Lambda}{\delta} + \sigma^2\frac{\Lambda^2}{\delta^2}\right)^2}{4\Lambda} - \left(\delta + \beta\frac{\Lambda}{\delta} + \sigma^2\frac{\Lambda^2}{\delta^2}\right)\mathbb{E}[\mathcal{S}^{-1}].$$

The equilibrium yields:

$$\limsup_{t\to\infty} \mathbb{E}[\mathcal{S}^{-1}(t)] \leq \frac{\delta + \frac{\beta\Lambda}{\delta} + \frac{\sigma^2\Lambda^2}{\delta^2}}{\Lambda}.$$

Remark 1. *From Proposition 2 and Jensen's inequality:*

$$\liminf_{t\to\infty} \mathbb{E}[\mathcal{S}(t)] \geq \frac{\Lambda}{\delta + \frac{\beta\Lambda}{\delta} + \frac{\sigma^2\Lambda^2}{\delta^2}},$$

a weaker bound than Proposition 1, but useful for later analysis.

Proposition 3. *Under condition* (3)*, for* $(\mathcal{S}(0), \mathcal{I}(0)) \in \mathcal{D}$*:*

$$\limsup_{t\to\infty} \mathbb{E}\left[\left(\frac{\Lambda}{\delta} - \mathcal{S}(t) - \mathcal{I}(t)\right)^{-\theta}\right] \leq m_\theta,$$

where θ *satisfies:*

$$\theta < \frac{2}{\sigma^2}\left(\xi + \beta\frac{\Lambda}{\delta}\right),$$

and $m_\theta > 0$ *is determined below.*

Proof. Let $\mathcal{Z} = \mathcal{S} + \mathcal{I}$. From (1):

$$\frac{d}{dt}\left(\frac{\Lambda}{\delta} - \mathcal{Z}\right)^{-\theta} = \theta\delta\left(\frac{\Lambda}{\delta} - \mathcal{Z}\right)^{-\theta} - \theta\left(\gamma + \epsilon + \frac{\alpha}{\lambda + \mathcal{I}}\right)\mathcal{I}\left(\frac{\Lambda}{\delta} - \mathcal{Z}\right)^{-\theta-1}.$$

Since $\mathcal{I} \leq \frac{\Lambda}{\delta}$:

$$\frac{d}{dt}\left(\frac{\Lambda}{\delta} - \mathcal{Z}\right)^{-\theta} \leq \delta(\theta+1)\left(\frac{\Lambda}{\delta} - \mathcal{Z}\right)^{-\theta} - \theta\left(\gamma + \epsilon + \frac{\alpha}{\lambda + \frac{\Lambda}{\delta}}\right)\mathcal{I}\left(\frac{\Lambda}{\delta} - \mathcal{Z}\right)^{-\theta-1}.$$

Using the inequality $a(\theta+1)x^{-\theta} - bx^{-\theta-1} \leq \frac{a^{\theta+1}}{b^\theta}$:

$$\frac{d}{dt}\left(\frac{\Lambda}{\delta} - \mathcal{Z}\right)^{-\theta} \leq \frac{\delta^{\theta+1}\mathcal{I}^{-\theta}}{\left(\gamma + \epsilon + \frac{\alpha}{\lambda + \frac{\Lambda}{\delta}}\right)^\theta} - \delta\left(\frac{\Lambda}{\delta} - \mathcal{Z}\right)^{-\theta}.$$

Taking expectations:

$$\frac{d}{dt}\mathbb{E}\left[\left(\frac{\Lambda}{\delta} - \mathcal{Z}\right)^{-\theta}\right] \leq \frac{\delta^{\theta+1}\mathbb{E}[\mathcal{I}^{-\theta}]}{\left(\gamma + \epsilon + \frac{\alpha}{\lambda + \frac{\Lambda}{\delta}}\right)^\theta} - \delta\mathbb{E}\left[\left(\frac{\Lambda}{\delta} - \mathcal{Z}\right)^{-\theta}\right].$$

From Theorem 1:

$$\limsup_{t\to\infty} \mathbb{E}[\mathcal{I}^{-\theta}(t)] \leq \frac{\kappa_1}{\kappa_2}.$$

Thus:

$$\limsup_{t\to\infty} \mathbb{E}\left[\left(\frac{\Lambda}{\delta} - \mathcal{Z}\right)^{-\theta}\right] \leq \frac{\delta^\theta \frac{\kappa_1}{\kappa_2}}{\left(\gamma + \epsilon + \frac{\alpha}{\lambda + \frac{\Lambda}{\delta}}\right)^\theta} \triangleq m_\theta.$$

To explore the asymptotic distribution, we analyze the transition probability function:

$$P(t, s_0, i_0, B) = \mathbb{P}((\mathcal{S}(t), \mathcal{I}(t)) \in B \mid \mathcal{S}(0) = s_0, \mathcal{I}(0) = i_0),$$

for $B \in \mathcal{B}(\mathcal{D})$, the Borel σ-algebra on $\mathcal{D}$.

Proposition 4. *For all $t > 0$, $(s_0, i_0) \in \mathcal{D}$, the transition probability $P(t, s_0, i_0, \cdot)$ has a smooth density $\pi(t, s, i, s_0, i_0) \in C^\infty(\mathbb{R}_+ \times \mathcal{D} \times \mathcal{D})$.*

Proof. Rewrite (1) in Stratonovich form:

$$\begin{cases} d\mathcal{S} = \left(\Lambda - \frac{\beta \mathcal{S}\mathcal{I}}{1+k\mathcal{I}} - \delta\mathcal{S} + \frac{\sigma^2 \mathcal{S}\mathcal{I}(\mathcal{S}-\mathcal{I})}{2(1+k\mathcal{I})^2}\right) dt - \frac{\sigma \mathcal{S}\mathcal{I}}{1+k\mathcal{I}} \circ dB, \\ d\mathcal{I} = \left(\frac{\beta \mathcal{S}\mathcal{I}}{1+k\mathcal{I}} - (\delta + \gamma + \epsilon)\mathcal{I} - \frac{\alpha \mathcal{I}}{\lambda + \mathcal{I}} - \frac{\sigma^2 \mathcal{S}\mathcal{I}(\mathcal{S}-\mathcal{I})}{2(1+k\mathcal{I})^2}\right) dt + \frac{\sigma \mathcal{S}\mathcal{I}}{1+k\mathcal{I}} \circ dB. \end{cases}$$

Define vector fields:

$$a(s,i) = \begin{pmatrix} \Lambda - \frac{\beta si}{1+ki} - \delta s + \frac{\sigma^2 si(s-i)}{2(1+ki)^2} \\ \frac{\beta si}{1+ki} - (\delta + \gamma + \epsilon)i - \frac{\alpha i}{\lambda + i} - \frac{\sigma^2 si(s-i)}{2(1+ki)^2} \end{pmatrix}, \quad b(s,i) = \begin{pmatrix} -\frac{\sigma si}{1+ki} \\ \frac{\sigma si}{1+ki} \end{pmatrix}.$$

Compute the Lie bracket $[a, b]$ and evaluate:

$$\det([a,b], b) = \left(\frac{\sigma si}{1+ki}\right)^2 \left(\gamma + \epsilon + \frac{\alpha\lambda}{(\lambda + i)^2}\right) > 0,$$

for $(s, i) \in \mathcal{D}$. Thus, $[a, b]$ and b span $\mathbb{R}^2$. By Hörmander's theorem [35], the transition probability has a smooth density.

Theorem 2. *For any $(s_0, i_0), (s_1, i_1) \in \mathcal{D}$, there exists $T > 0$ such that:*

$$\pi(T, s_1, i_1 \mid s_0, i_0) > 0.$$

Proof. Consider the control system:

$$\begin{cases} \frac{d\mathcal{S}_\varphi}{dt} = a_1(\mathcal{S}_\varphi, \mathcal{I}_\varphi) + b_1(\mathcal{S}_\varphi, \mathcal{I}_\varphi)\varphi, \\ \frac{d\mathcal{I}_\varphi}{dt} = a_2(\mathcal{S}_\varphi, \mathcal{I}_\varphi) + b_2(\mathcal{S}_\varphi, \mathcal{I}_\varphi)\varphi, \end{cases}$$

with $\mathcal{S}_\varphi(0) = s_0$, $\mathcal{I}_\varphi(0) = i_0$, and coefficients from Proposition 4. Define $\mathcal{Z}_\varphi = \mathcal{S}_\varphi + \mathcal{I}_\varphi$:

$$\frac{d\mathcal{Z}_\varphi}{dt} = \Lambda - \delta\mathcal{Z}_\varphi - (\gamma + \epsilon)\mathcal{I}_\varphi - \frac{\alpha \mathcal{I}_\varphi}{\lambda + \mathcal{I}_\varphi}.$$

Construct a trajectory from (s_0, i_0) to (s_1, i_1). Define:

$$\mathcal{Z}_1(t) = \mathcal{Z}(t) + \frac{g(z_0) - g(i_0)}{g(z_0)}(\bar{\mathcal{Z}}(t) - \mathcal{Z}(t)),$$

where $\mathcal{Z}, \bar{\mathcal{Z}}$ solve:

$$\frac{d\mathcal{Z}}{dt} = \psi(\mathcal{Z}), \quad \frac{d\bar{\mathcal{Z}}}{dt} = \Lambda - \delta\bar{\mathcal{Z}},$$

with $\mathcal{Z}(0) = \bar{\mathcal{Z}}(0) = z_0 = s_0 + i_0$, and $g(x) = (\gamma + \epsilon)x + \frac{\alpha x}{\lambda + x}$. Then:

$$\mathcal{Z}_1(0) = z_0, \quad \frac{d\mathcal{Z}_1}{dt}(0) = \Lambda - \delta z_0 - g(i_0).$$

Since g is increasing and $\psi(\mathcal{Z}_1) < \frac{d\mathcal{Z}_1}{dt} < \Lambda - \delta\mathcal{Z}_1$, $\mathcal{Z}_1(t) \in (z^*, \Lambda/\delta)$. Similarly, define:

$$\mathcal{Z}_3(t) = \bar{\mathcal{Z}}(t) + \frac{g(z_1) - g(i_1)}{g(z_1)}(\bar{\mathcal{Z}}(T-t) - \mathcal{Z}(T-t)),$$

with $\mathcal{Z}_3(T) = z_1 = s_1 + i_1$. Choose $\mathcal{Z}_2(t)$ on $[\eta, T-\eta]$ such that $\mathcal{Z}_\varphi(t) = \mathcal{Z}_1(t), \mathcal{Z}_2(t), \mathcal{Z}_3(t)$ is C^1. Set:

$$\mathcal{I}_\varphi(t) = g^{-1}\left(\Lambda - \delta\mathcal{Z}_\varphi - \frac{d\mathcal{Z}_\varphi}{dt}\right),$$

and compute φ. This trajectory connects (s_0, i_0) to (s_1, i_1), ensuring positive density by support theorems [35].

Theorem 3. *Under condition* (3)*, for* $(s_0, i_0) \in \mathcal{D}$*, there exists a compact set* $\mathcal{K} \subset \mathcal{D}$ *such that:*

$$\liminf_{t\to\infty} \frac{1}{t}\int_0^t P(u, (s_0, i_0), \mathcal{K})du > 0,$$

and a unique stationary density π^* *satisfying:*

$$\lim_{t\to\infty}\int_{\mathcal{D}} |\pi(t, x, (s_0, i_0)) - \pi^*(x)|dx = 0.$$

Proof. Let $\mathcal{Z} = \mathcal{S} + \mathcal{I}$. From (1):

$$\frac{d\mathcal{Z}}{dt} \geq \psi(\mathcal{Z}).$$

Choose $h > 0$ small such that $\psi(z^* + h) < -(\gamma + \epsilon)m_S$, where $m_S = \frac{\Lambda}{\delta + \frac{\beta\Lambda}{\delta}}$. By Proposition 1:

$$\liminf_{t\to\infty} \frac{1}{t}\int_0^t -\psi(\mathcal{Z}(u))du \geq (\gamma + \epsilon)m_S.$$

Using Hölder's inequality:

$$\frac{1}{t}\int_0^t -\mathbb{1}_{\{\mathcal{Z}(u)\geq z^*+h\}}\psi(\mathcal{Z}(u))du \leq -\psi\left(\frac{\Lambda}{\delta}\right)\left(\frac{1}{t}\int_0^t \mathbb{1}_{\{\mathcal{Z}(u)\geq z^*+h\}}du\right)^{1/2}.$$

Thus:

$$\liminf_{t\to\infty} \frac{1}{t}\int_0^t \mathbb{1}_{\{\mathcal{Z}(u)\geq z^*+h\}}du \geq \left[\psi\left(\frac{\Lambda}{\delta}\right)\right]^{-2}\left[(\gamma + \epsilon)m_S + \psi(z^* + h)\right]^2.$$

Define sets:

$$\mathcal{K}_1 = \{(s,i) : s+i \geq z^* + h\}, \quad \mathcal{K}_2 = \{s \geq h_2\}, \quad \mathcal{K}_3 = \{i \geq h_3\}, \quad \mathcal{K}_4 = \{s+i \leq \frac{\Lambda}{\delta} - h_4\}.$$

Using Propositions 2, 3, and Markov's inequality, choose h_2, h_3, h_4 to ensure:

$$\liminf_{t\to\infty} \frac{1}{t} \int_0^t P(u, (s_0, i_0), \mathcal{K}_i) du \geq 1 - \text{small terms}.$$

Set $\mathcal{K} = \bigcap_{i=1}^4 \mathcal{K}_i$. Then:

$$\liminf_{t\to\infty} \frac{1}{t} \int_0^t P(u, (s_0, i_0), \mathcal{K}) du > 0.$$

By Proposition 4 and Theorem 2, the Markov semigroup is asymptotically stable [35], yielding a unique π^*.

3. Conditions for Disease Elimination

Recent studies on stochastic extinction conditions, such as in SEIR models with delays and noise [36] and SIVR models with vaccination perturbations [37], provide context for our analysis of disease elimination under resource constraints. We investigate the long-term dynamics of a stochastic epidemic model governing susceptible ($\mathcal{S}(t)$) and infected ($\mathcal{I}(t)$) populations, initialized at $x_0 = (s_0, i_0) \in \mathbb{R}^2_+$, where:

$$\mathbb{R}^2_+ = \{(s,i) \in \mathbb{R}^2 : s > 0, i > 0\}.$$

Prior analysis (analogous to earlier lemmas) guarantees that the solution $(\mathcal{S}(t), \mathcal{I}(t))$ remains in $\mathbb{R}^2_+$ with probability 1. Furthermore, employing techniques similar to those establishing invariant regions, we identify a compact, positively invariant, and attractive set:

$$\mathcal{A} = \left\{ (s,i) \in \mathbb{R}^2_+ : x^* \leq s+i \leq \frac{\Lambda}{\delta} \right\},$$

where x^* is the unique root of the function $\phi(x) = \Lambda - (\delta + \gamma + \epsilon)x - \frac{\alpha x}{\lambda + x}$. Consequently, we restrict our study of the system's asymptotic behavior to the state space $\mathcal{A}$.

In this section, we derive conditions ensuring disease extinction by examining the stability of the disease-free equilibrium $E_0 = \left(\frac{\Lambda}{\delta}, 0\right)$. We denote the solution with initial condition $x_0 = (s_0, i_0) \in \mathcal{A}$ as $\mathcal{X}^{x_0}(t) = (\mathcal{S}(t), \mathcal{I}(t))$, and use $\mathcal{X}^{u,x}(t)$ to indicate the solution satisfying $\mathcal{X}(u) = x$. The Euclidean norm in $\mathbb{R}^2$ is denoted by $\|\cdot\|$. Drawing on stochastic stability theory [38, 39], we establish an almost necessary and sufficient condition for the disease to vanish, as formalized below.

Theorem 4. *Assume the parameter condition:*

$$\eta \triangleq \frac{\beta\Lambda}{\delta} - \left(\delta + \gamma + \epsilon + \frac{\alpha}{\lambda} + \frac{1}{2} \left(\frac{\sigma\Lambda}{\delta} \right)^2 \right) < 0. \tag{4}$$

Then, the disease-free equilibrium $E_0 = \left(\frac{\Lambda}{\delta}, 0\right)$ *is asymptotically stable in the large in the stochastic sense. Specifically,* E_0 *is stochastically stable, and for all initial conditions* $x_0 = (s_0, i_0) \in \mathcal{A}$*:*

$$\mathbb{P}\left(\lim_{t\to\infty} \mathcal{X}^{x_0}(t) = E_0\right) = 1.$$

Proof. To demonstrate asymptotic stability, we follow the approach outlined in [38] , which equates the stability of the nonlinear system to that of its linearization at E_0. Introduce transformed variables:

$$\mathcal{X}_1 = \frac{\Lambda}{\delta} - \mathcal{S}, \quad \mathcal{X}_2 = \mathcal{I}.$$

Linearizing the system around E_0, we obtain:

$$\begin{cases} d\mathcal{X}_1 = \left(-\delta\mathcal{X}_1 + \frac{\beta\Lambda}{\delta}\mathcal{X}_2\right) dt + \frac{\sigma\Lambda}{\delta}\mathcal{X}_2 dB(t), \\ d\mathcal{X}_2 = \left[\frac{\beta\Lambda}{\delta} - \left(\delta + \gamma + \epsilon + \frac{\alpha}{\lambda}\right)\right] \mathcal{X}_2 dt + \frac{\sigma\Lambda}{\delta}\mathcal{X}_2 dB(t). \end{cases} \tag{5}$$

Define a positive-definite Lyapunov function:

$$\psi(\mathcal{X}_1, \mathcal{X}_2) = k\mathcal{X}_1 + \frac{1}{p}\mathcal{X}_2^p, \tag{6}$$

where $k, p > 0$ are parameters to be chosen. Let $\mathcal{L}$ be the infinitesimal generator associated with (5). Compute:

$$\mathcal{L}\psi = k\left(-\delta\mathcal{X}_1 + \frac{\beta\Lambda}{\delta}\mathcal{X}_2\right) + \mathcal{X}_2^{p-1}\left[\frac{\beta\Lambda}{\delta} - \left(\delta + \gamma + \epsilon + \frac{\alpha}{\lambda}\right)\right] + \frac{p(p-1)}{2}\left(\frac{\sigma\Lambda}{\delta}\right)^2 \mathcal{X}_2^{p-2} \cdot \mathcal{X}_2^2.$$

Simplify the stochastic term:

$$\frac{p(p-1)}{2}\left(\frac{\sigma\Lambda}{\delta}\right)^2 \mathcal{X}_2^{p-2} \cdot \mathcal{X}_2^2 = \frac{p(p-1)}{2}\left(\frac{\sigma\Lambda}{\delta}\right)^2 \mathcal{X}_2^p.$$

Thus:

$$\mathcal{L}\psi = -k\delta\mathcal{X}_1 + k\frac{\beta\Lambda}{\delta}\mathcal{X}_2 + \left[\frac{\beta\Lambda}{\delta} - \left(\delta + \gamma + \epsilon + \frac{\alpha}{\lambda}\right) + \frac{p(p-1)}{2}\left(\frac{\sigma\Lambda}{\delta}\right)^2\right] \mathcal{X}_2^p.$$

Since:

$$\frac{p(p-1)}{2} = \frac{p^2 - p}{2} = \frac{p}{2}(p-1) \leq \frac{p}{2} \cdot 0 = 0 \quad \text{for } p \in (0, 1),$$

and noting that:

$$\frac{\beta\Lambda}{\delta} - \left(\delta + \gamma + \epsilon + \frac{\alpha}{\lambda}\right) = \eta + \frac{1}{2}\left(\frac{\sigma\Lambda}{\delta}\right)^2,$$

we rewrite:

$$\mathcal{L}\psi = -k\delta\mathcal{X}_1 + k\frac{\beta\Lambda}{\delta}\mathcal{X}_2 + \left[\eta + \frac{1}{2}\left(\frac{\sigma\Lambda}{\delta}\right)^2 + \frac{p(p-1)}{2}\left(\frac{\sigma\Lambda}{\delta}\right)^2\right] \mathcal{X}_2^p.$$

Combine terms:

$$\frac{1}{2}\left(\frac{\sigma\Lambda}{\delta}\right)^2+\frac{p(p-1)}{2}\left(\frac{\sigma\Lambda}{\delta}\right)^2=\frac{1}{2}\left(\frac{\sigma\Lambda}{\delta}\right)^2[1+p(p-1)]=\frac{1}{2}\left(\frac{\sigma\Lambda}{\delta}\right)^2 p.$$

Thus:

$$\mathcal{L}\psi=-k\delta\mathcal{X}_1+k\frac{\beta\Lambda}{\delta}\mathcal{X}_2+\left[\eta+\frac{1}{2}p\left(\frac{\sigma\Lambda}{\delta}\right)^2\right]\mathcal{X}_2^p. \tag{7}$$

Since $\eta<0$ by (4), select $p\in(0,1)$ such that:

$$\eta+\frac{1}{2}p\left(\frac{\sigma\Lambda}{\delta}\right)^2<0.$$

This is feasible, as choosing p small ensures the positive term $\frac{1}{2}p\left(\frac{\sigma\Lambda}{\delta}\right)^2$ does not dominate η. Next, choose $k>0$ to satisfy:

$$\eta+\frac{1}{2}p\left(\frac{\sigma\Lambda}{\delta}\right)^2+k\frac{\beta\Lambda}{\delta}<0. \tag{8}$$

For small $\mathcal{X}_2$, since $p<1$, $\mathcal{X}_2^p>\mathcal{X}_2$, so:

$$k\frac{\beta\Lambda}{\delta}\mathcal{X}_2\le\left[k\frac{\beta\Lambda}{\delta}\right]\mathcal{X}_2^p.$$

Thus:

$$\mathcal{L}\psi\le-k\delta\mathcal{X}_1+\left[\eta+\frac{1}{2}p\left(\frac{\sigma\Lambda}{\delta}\right)^2+k\frac{\beta\Lambda}{\delta}\right]\mathcal{X}_2^p.$$

By (8), the coefficient of $\mathcal{X}_2^p$ is negative, and since $\mathcal{X}_1\ge0$ in $\mathcal{A}$, we have:

$$\mathcal{L}\psi\le0.$$

Per [39] , this implies stochastic stability of the origin $(0,0)$ for (5). Hence, for any $\varepsilon>0$ and $r>0$, there exists $d>0$ such that:

$$\mathbb{P}\left(\sup_{t\ge0}\|\mathcal{X}^{x_0}(t)-E_0\|<r\right)\ge1-\varepsilon,\quad\forall x_0\in\tilde{B}_d, \tag{9}$$

where:

$$\tilde{B}_d=\left\{x\in\overline{\mathcal{A}}:\|x-E_0\|\le d\right\}.$$

To extend stability to global convergence, consider any $x\in\overline{\mathcal{A}}$. By prior results on connectivity (cf. Theorem 2.2 in earlier sections), there exists $T_x>0$ such that:

$$P(T_x,x,\tilde{B}_d)\ge p_x>0. \tag{10}$$

The process $\mathcal{X}(t)$ possesses the Feller property, as established by the smoothness of its transition density (cf. Proposition 3). Thus, there exists an open neighborhood $\mathcal{V}_x \subset \overline{\mathcal{A}}$ of x such that:

$$P(T_x, y, \tilde{B}_d) \geq p_x > 0, \quad \forall y \in \mathcal{V}_x. \tag{11}$$

Since $\overline{\mathcal{A}}$ is compact, there exists a finite cover:

$$\overline{\mathcal{A}} \subset \bigcup_{i=1}^{m} \mathcal{V}_{x_i}, \tag{12}$$

for some $x_i \in \overline{\mathcal{A}}$, $i = 1, \ldots, m$. Define:

$$T^* = \max_{1 \leq i \leq m} T_{x_i}, \quad p^* = \min_{1 \leq i \leq m} p_{x_i}.$$

For any initial condition $x_0 \in \overline{\mathcal{A}}$, combining (11) and (12):

$$P(T^*, x_0, \tilde{B}_d) \geq p^* > 0. \tag{13}$$

Introduce the stopping time:

$$\tau^{x_0} = \inf \left\{ t \geq 0 : \mathcal{X}^{x_0}(t) \in \tilde{B}_d \right\}.$$

Define a sequence of times:

$$\nu_n^{x_0} = \inf \left\{ t \in [(n-1)T^*, nT^*] : \mathcal{X}^{x_0}(t) \in \tilde{B}_d \right\},$$

with the convention $\inf \emptyset = \infty$. The probability that the process never enters $\tilde{B}_d$ is:

$$\mathbb{P}\left(\tau^{x_0} = \infty\right) = \mathbb{P}\left(\nu_n^{x_0} = \infty, \ \forall n \geq 1\right) = \lim_{k \to \infty} \mathbb{P}\left(\bigcap_{n=1}^{k} \nu_n^{x_0} = \infty \right).$$

Compute:

$$\mathbb{P}\left(\bigcap_{n=1}^{k} \nu_n^{x_0} = \infty \right) = \mathbb{P}\left(\nu_1^{x_0} = \infty\right) \prod_{n=2}^{k} \mathbb{P}\left(\nu_n^{x_0} = \infty \mid \nu_{n-1}^{x_0} = \infty\right). \tag{14}$$

From (13):

$$\mathbb{P}\left(\nu_1^{x_0} = \infty\right) = \mathbb{P}\left(\mathcal{X}^{x_0}(t) \notin \tilde{B}_d, \ \forall t \in [0, T^*] \right) \leq 1 - p^*.$$

For $n \geq 2$, by the Markov property:

$$\mathbb{P}\left(\nu_n^{x_0} = \infty \mid \nu_{n-1}^{x_0} = \infty\right) = \mathbb{P}\left(\mathcal{X}^{x_0}(t) \notin \tilde{B}_d, \ \forall t \in [(n-1)T^*, nT^*] \mid \mathcal{X}^{x_0}(t) \notin \tilde{B}_d, \ \forall t \in [(n-2)T^*, (n-1)T^*] \right).$$

Conditioning on $\mathcal{X}^{x_0}((n-1)T^*)$:

$$\mathbb{P}\left(\mathcal{X}^{x_0}(t) \notin \tilde{B}_d, \ \forall t \in [(n-1)T^*, nT^*] \mid \mathcal{X}^{x_0}((n-1)T^*) = x \right) = \mathbb{P}\left(\mathcal{X}^{0,x}(s) \notin \tilde{B}_d, \ \forall s \in [0, T^*] \right) \leq 1 - p^*,$$

since $P(T^*, x, \tilde{B}_d) \geq p^*$. Thus:

$$\mathbb{P}\left(\nu_n^{x_0} = \infty \mid \nu_{n-1}^{x_0} = \infty\right) \leq \int_{\overline{\mathcal{A}}} \mathbb{P}\left(\mathcal{X}^{0,x}(s) \notin \tilde{B}_d,\ \forall s \in [0, T^*]\right) \pi((n-1)T^*, x, x_0)\, dx \leq 1 - p^*.$$

Substituting into (14):

$$\mathbb{P}\left(\bigcap_{n=1}^{k} \nu_n^{x_0} = \infty\right) \leq (1 - p^*)^k.$$

As $k \to \infty$, $(1 - p^*)^k \to 0$, so:

$$\mathbb{P}\left(\tau^{x_0} = \infty\right) = 0, \quad \text{i.e.,} \quad \mathbb{P}\left(\tau^{x_0} < \infty\right) = 1.$$

By the strong Markov property and (9), for any $r, \varepsilon > 0$:

$$\mathbb{P}\left(\limsup_{t\to\infty} \|\mathcal{X}^{x_0}(t) - E_0\| > r\right) = \mathbb{E}\left[\mathbb{P}\left(\limsup_{t\to\infty} \|\mathcal{X}^{x_0}(t) - E_0\| > r \mid \mathcal{F}_{\tau^{x_0}}\right)\right].$$

At τ^{x_0}, $\mathcal{X}^{x_0}(\tau^{x_0}) \in \tilde{B}_d$, so:

$$\mathbb{P}\left(\limsup_{t\to\infty} \|\mathcal{X}^{\tau^{x_0},x}(t) - E_0\| > r\right) \leq \varepsilon, \quad \forall x \in \tilde{B}_d.$$

Thus:

$$\mathbb{P}\left(\limsup_{t\to\infty} \|\mathcal{X}^{x_0}(t) - E_0\| > r\right) \leq \int_0^\infty \int_{\tilde{B}_d} \mathbb{P}\left(\limsup_{t\to\infty} \|\mathcal{X}^{u,x}(t) - E_0\| > r\right) \mathbb{P}(\tau^{x_0} \in du, \mathcal{X}^{x_0}(\tau^{x_0}) \in dx) \leq \varepsilon.$$

Since ε and r are arbitrary:

$$\mathbb{P}\left(\limsup_{t\to\infty} \|\mathcal{X}^{x_0}(t) - E_0\| > 0\right) = 0,$$

implying:

$$\mathbb{P}\left(\lim_{t\to\infty} \mathcal{X}^{x_0}(t) = E_0\right) = 1.$$

This completes the proof.

4. Numerical Analysis and Dynamics

To elucidate the impact of stochastic perturbations on epidemic dynamics, we compare our findings with a deterministic model analyzed in prior work [40–43]. That study explored the global behavior of the deterministic system (denoted as equation (1.1)) across three parameter regions defined by λ and α:

$$\mathcal{O}_1 = \left\{(\lambda, \alpha) : \lambda \geq \frac{\delta}{\beta + \delta k}, \alpha > 0\right\},$$
$$\mathcal{O}_2 = \left\{(\lambda, \alpha) : 0 < \lambda < \frac{\delta}{\beta + \delta k}, 0 < \alpha \leq \alpha_0(\lambda)\right\},$$

$$\mathcal{O}_3 = \left\{ (\lambda, \alpha) : 0 < \lambda < \frac{\delta}{\beta + \delta k}, \alpha > \alpha_0(\lambda) \right\},$$

where the threshold is:

$$\alpha_0(\lambda) = \frac{\lambda^2(\beta + \delta k)(\delta + \gamma + \epsilon)}{\delta - \lambda(\beta + \delta k)}.$$

The analysis revealed rich dynamics: a forward bifurcation at $\mathcal{R}_0 = 1$ for $(\lambda, \alpha) \in \mathcal{O}_1 \cup \mathcal{O}_2$, and a backward bifurcation in $\mathcal{O}_3$ when $P^* < \mathcal{R}_0 < 1$, transitioning from the disease-free equilibrium to two endemic equilibria, with P^* defined in [40–43].

We present three numerical examples to illustrate how stochasticity alters these dynamics, focusing on system (1.2), a stochastic extension of (1.1). Simulations visualize trajectories and bifurcation surfaces, highlighting extinction, persistence, and parameter-driven transitions.

4.1. Example 1: Stochastic Extinction in Backward Bifurcation Regime

In the deterministic setting, when $(\lambda, \alpha) \in \mathcal{O}_3$ and $P^* < \mathcal{R}_0 < 1$, the system exhibits a backward bifurcation, with a disease-free equilibrium E_0, a saddle-point endemic equilibrium E_1, and a stable endemic equilibrium E_2. Introducing noise can destabilize the endemic state, driving trajectories toward extinction.

Consider the deterministic system (1.1) with parameters:

$$\beta = 0.0048, \quad \Lambda = 15, \quad \alpha = 6.5, \quad \lambda = 6.8, \quad k = 0.012, \quad \delta = 0.09, \quad \gamma = 0.015, \quad \epsilon = 0.025.$$

Calculating the basic reproduction number yields $\mathcal{R}_0 = 0.82$, and the threshold $P^* = 0.78$, confirming the presence of E_0, E_1, and E_2.

The threshold $P^* = 0.78$ represents the critical value for backward bifurcation in the deterministic model, below which multiple endemic equilibria exist when $\mathcal{R}_0 < 1$, highlighting subcritical persistence.

Now, we simulate the stochastic system (1.2) with the same parameters and noise intensity $\sigma = 0.0018$. This yields:

$$\eta = \frac{\beta\Lambda}{\delta} - \left(\delta + \gamma + \epsilon + \frac{\alpha}{\lambda} + \frac{1}{2} \left(\frac{\sigma\Lambda}{\delta} \right)^2 \right) = -0.22 < 0,$$

satisfying Theorem 4. Figure 1 compares deterministic and stochastic trajectories, showing the stochastic system converging to E_0, unlike the deterministic case, which stabilizes at E_2.

4.2. Example 2: Bifurcation Surfaces Under Stochasticity

To explore the influence of parameters λ and α on the infected population, we analyze system (1.2) with:

$$\beta = 0.009, \quad \Lambda = 15, \quad k = 0.0015, \quad \delta = 0.095, \quad \gamma = 0.11, \quad \epsilon = 0.18, \quad \sigma = 0.0015.$$

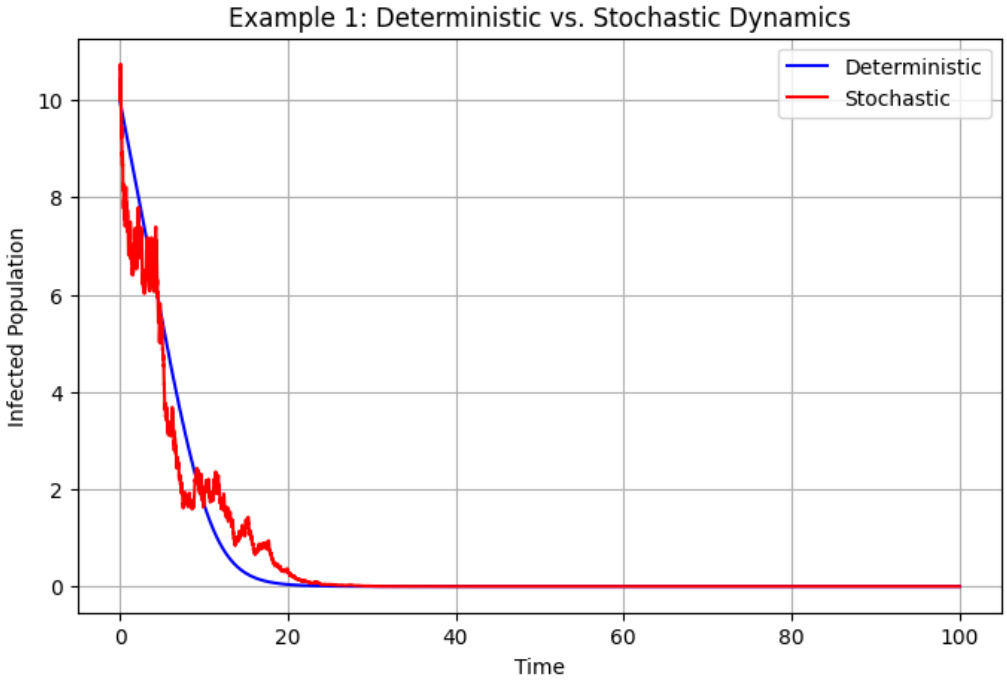

Figure 1: Comparison of deterministic and stochastic dynamics for Example 1. The deterministic trajectory (blue) converges to the endemic equilibrium E_2, while the stochastic trajectory (red) approaches the disease-free equilibrium E_0, illustrating Theorem 4 with $\eta = -0.25 < 0$.

Bifurcation analysis reveals how λ and α shape the long-term infected population size. We generate bifurcation surfaces for both deterministic (1.1) and stochastic (1.2) systems, varying $\lambda \in [1, 10]$ and $\alpha \in [0, 10]$.

Figure 2a shows the deterministic bifurcation surface, displaying regions of extinction and persistence, with transitions corresponding to $\mathcal{R}_0 = 1$. Figure 2b presents the stochastic counterpart, where noise smooths transitions and expands the extinction region, highlighting stochasticity's role in epidemic control.

4.3. Example 3: Extinction vs. Persistence

We demonstrate the implications of Theorems 1 and 4 by considering the parameters:

$$\Lambda = 15, \quad \delta = 0.09, \quad \gamma = 0.015, \quad \epsilon = 0.025, \quad k = 0.012, \quad \beta = 0.0028,$$

with $(\alpha, \lambda) \in \mathcal{O}_1 \cup \mathcal{O}_2$, and noise levels $\sigma \in \{0.001, 0.003\}$. For $\sigma = 0.001$, $\eta = 0.20 > 0$, showing persistence (Figure 3b). For $\sigma = 0.003$, $\eta = -0.20 < 0$, showing extinction (Figure 3a).

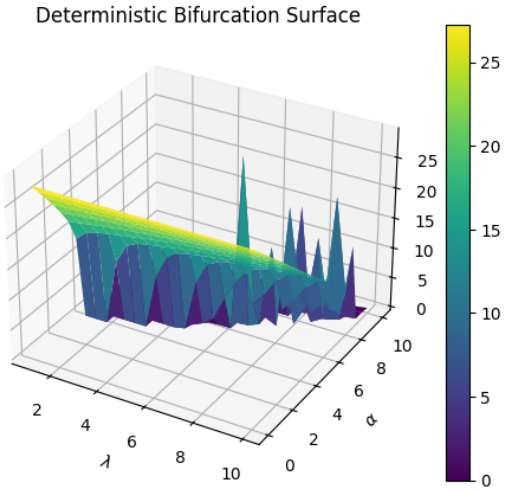

(a) Deterministic bifurcation surface for the infected population as a function of λ and α. Sharp transitions indicate bifurcation boundaries.

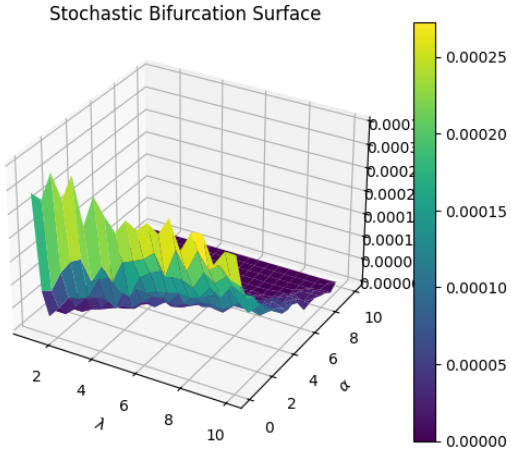

(b) Stochastic bifurcation surface, showing smoothed transitions and an expanded extinction region due to noise ($\sigma = 0.0015$).

Figure 2: Bifurcation surfaces for Example 2, comparing deterministic and stochastic dynamics of system (1.2).

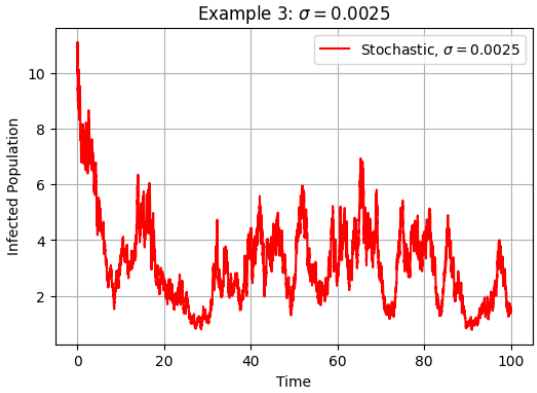

(a) Disease extinction with $\sigma = 0.0025$, $\eta = -0.18 < 0$, per Theorem 4.

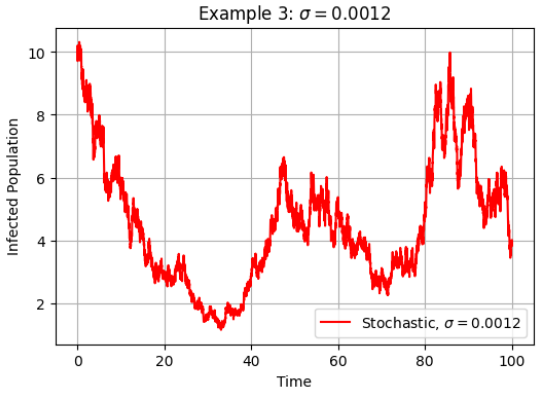

(b) Disease persistence with $\sigma = 0.0012$, $\eta = 0.15 > 0$, per Theorem 1.

Figure 3: Stochastic trajectories for Example 3, illustrating extinction and persistence under different noise levels.

5. Summary and Outlook

This study explored the dynamics of a stochastic SIR epidemic model with nonlinear incidence, limited medical resources, and environmental noise. Theoretical analysis established conditions for persistence, ergodicity, and extinction, while numerical simulations demonstrated noise's role in eliminating backward and Hopf bifurcations common in deterministic counterparts.

Our findings underscore how resource constraints shape epidemic trajectories under stochasticity, providing actionable insights for public health. Incorporating randomness enhances model realism, aiding adaptive strategies in uncertain environments.

Future work should extend the model to include spatial diffusion, time delays, heterogeneous populations, and evolving pathogens. Empirical validation with real-world data, such as from recent outbreaks, will refine parameters and align predictions with observed dynamics, fostering effective interventions.

Funding

This research was supported by University of Phayao and Thailand Science Research and Innovation Fund (Fundamental Fund 2026, Grant No. XXXX/2568).

Author Contributions: The authors equally conceived of the study, participated in its design and coordination, drafted the manuscript, participated in the sequence alignment, and read and approved the final manuscript.

Conflicts of Interest: The authors declare that they have no competing interests.

References

[1] H.W. Hethcote. Qualitative analyses of communicable disease models. *Mathematical biosciences*, 28(3-4):335–356, 1976.

[2] Y. Cai, J. Jiao, Z. Gui, Y. Liu, and W. Wang. Environmental variability in a stochastic epidemic model. *Applied Mathematics and Computation*, 329:210–226, 2018.

[3] J. Muhammad, U. Younas, N. Nasreen, A. Khan, and T. Abdeljawad. Multicomponent nonlinear fractional schrödinger equation: On the study of optical wave propagation in the fiber optics. *Partial Differential Equations in Applied Mathematics*, 11:100805, 2024.

[4] F. Brauer, C. Castillo-Chavez, Z. Feng, F. Brauer, C. Castillo-Chavez, and Z. Feng. Simple compartmental models for disease transmission. In *Mathematical models in epidemiology*, pages 21–61. Springer, 2019.

[5] S. Hottovy and S.N. Stechmann. A spatiotemporal stochastic model for tropical precipitation and water vapor dynamics. *Journal of the Atmospheric Sciences*, 72(12):4721–4738, 2015.

[6] G. Lan, B. Song, and S. Yuan. Epidemic threshold and ergodicity of an seir model with vertical transmission under the telegraph noise. *Chaos, Solitons and Fractals*, 167:113017, 2023.

[7] W.O. Kermack and A.G. McKendrick. A contribution to the mathematical theory of epidemics. *Proceedings of the royal society of london. Series A, Containing papers of a mathematical and physical character*, 115(772):700–721, 1927.

[8] A.V. Arundel, E.M. Sterling, J.H. Biggin, and T.D. Sterling. Indirect health effects of relative humidity in indoor environments. *Environmental health perspectives*, 65:351–361, 1986.

[9] S.M. Ud-Dean. Structural explanation for the effect of humidity on persistence of airborne virus: seasonality of influenza. *Journal of Theoretical Biology*, 264(3):822–829, 2010.

[10] M.J. Keeling and P. Rohani. *Modeling infectious diseases in humans and animals*. Princeton university press, 2008.

[11] P. Barmpounakis and N. Demiris. Multiphasic stochastic epidemic models. *Journal of the Royal Statistical Society Series C: Applied Statistics*, 74(2):491–505, 2025.

[12] B. Boukanjime and M. Maama. Stochastic dynamics and probability analysis for a generalized epidemic model with environmental noise. *Chaos, Solitons & Fractals*, 199:116744, 2025.

[13] J. Song, W. Lv, X. Yang, and C. Zhang. A stochastic epidemic model with individual heterogeneity and mean-reverting ornstein–uhlenbeck process. *International Journal of Biomathematics*, page 2450035, 2024.

[14] L. Liu, Y. Zhang, Y. Tian, D. Wei, and Z. Huang. Sliding mode control for stochastic sir models with telegraph and lévy noise: Theory and applications. *Symmetry*, 17(6):963, 2025.

[15] P.J. Landrigan. Air pollution and health. *The Lancet Public Health*, 2(1):e4–e5, 2017.

[16] S.G. Al-Kindi, R.D. Brook, S. Biswal, and S. Rajagopalan. Environmental determinants of cardiovascular disease: lessons learned from air pollution. *Nature Reviews Cardiology*, 17(10):656–672, 2020.

[17] B.G. Armstrong. Effect of measurement error on epidemiological studies of environmental and occupational exposures. *Occupational and environmental medicine*, 55(10):651–656, 1998.

[18] C. Asbach, H. Kaminski, D. Von Barany, T.A. Kuhlbusch, C. Monz, N. Dziurowitz, J. Pelzer, K. Vossen, K. Berlin, S. Dietrich, and U.W.E. Götz. Comparability of portable nanoparticle exposure monitors. *Annals of occupational hygiene*, 56(5):606–621, 2012.

[19] E. van de Beek, J. Kerckhoffs, G. Hoek, G. Sterk, K. Meliefste, U. Gehring, and R. Vermeulen. Spatial and spatiotemporal variability of regional background ultrafine particle concentrations in the netherlands. *Environmental science and technology*, 55(2):1067–105, 2020.

[20] V. Capasso. *Mathematical Structures of Epidemic Systems*. Springer-Verlag Berlin Heidelberg, 2008.

[21] F. Brauer, C. Castillo-Chavez, and C. Castillo-Chavez. *Mathematical models in pop-*

ulation biology and epidemiology, volume 2. Springer New York, 2012.

[22] M. Lipsitch, Y.H. Grad, A. Sette, and S. Crotty. Cross-reactive memory t cells and herd immunity to sars-cov-2. *Nature Reviews Immunology*, 20(11):709–713, 2020.

[23] J.M. Dan, J. Mateus, Y. Kato, K.M. Hastie, E.D. Yu, C.E. Faliti, A. Grifoni, S.I. Ramirez, S. Haupt, A. Frazier, and C. Nakao. Immunological memory to sars-cov-2 assessed for up to 8 months after infection. *Science*, 371(6529):eabf4063, 2021.

[24] B.S. Graham, J.R. Mascola, and A.S. Fauci. Novel vaccine technologies: essential components of an adequate response to emerging viral diseases. *Jama*, 319(14):1431–1432, 2018.

[25] J. Yang, M. Zhou, and X. Li. Backward bifurcation of an age-structured epidemic model with partial immunity: the lyapunov–schmidt approach. *Applied Mathematics Letters*, 133:108292, 2022.

[26] M.R. Boyce and R. Katz. Community health workers and pandemic preparedness: current and prospective roles. *Frontiers in public health*, 7:62, 2019.

[27] M. Shammi, M. Bodrud-Doza, A.R.M.T. Islam, and M.M. Rahman. Strategic assessment of covid-19 pandemic in bangladesh: comparative lockdown scenario analysis, public perception, and management for sustainability. *Environment, Development and Sustainability*, 23:6148–6191, 2021.

[28] F. Carinci. Covid-19: preparedness, decentralisation, and the hunt for patient zero. *Bmj*, 368, 2020.

[29] D.R. Chaudhury. At current pace, bangladesh to end extreme poverty by 2021. *The Economic Times*, 2018.

[30] J.P. Aparicio, A.F. Capurro, and C. Castillo-Chavez. Transmission and dynamics of tuberculosis on generalized households. *Journal of theoretical biology*, 206(3):327–341, 2000.

[31] W. Miller, C. Castillo-Chavez, S. Blower, D. Kirschner, and A.A. Yakubu. *Mathematical approaches for emerging and reemerging infectious diseases: Models, methods, and theory*. Springer New York, 2002.

[32] J.P. Aparicio, A.F. Capurro, and C. Castillo-Chavez. Markers of disease evolution: the case of tuberculosis. *Journal of theoretical Biology*, 215(2):227–237, 2002.

[33] S.J. Aston. Pneumonia in the developing world: Characteristic features and approach to management. *Respirology*, 22(7):1276–1287, 2017.

[34] National Academies of Sciences, Engineering, and Medicine. *Quality measurement and quality improvement*. National Academies Press (US), 2022.

[35] L. Hörmander. Hypoelliptic second order differential operators. *Acta Mathematica*, 119(1):147–171, 1967.

[36] A. Khan and R. Zarin. A stochastic epidemic model with time delays and unreported cases: Uncertainty and sensitivity analyses. *Results in Control and Optimization*, 15:100475, 2024.

[37] X. Liu, Y. Takeuchi, and S. Iwami. Svir epidemic models with vaccination strategies. *Journal of Theoretical biology*, 253(1):1–11, 2008.

[38] B. Øksendal. *Stochastic Differential Equations: An Introduction with Applications*. Springer Berlin, 6th edition, 2003.

[39] X. Mao. *Stochastic Differential Equations and Applications*. Horwood Publishing Chichester, 1997.

[40] Q. Liu, D. Jiang, N. Shi, and T. Hayat. Dynamics of a stochastic sir epidemic model with saturated incidence and vaccination. *Mathematics and Computers in Simulation*, 205:1–26, 2023.

[41] Y. Zhou and W. Zhang. Threshold dynamics of a stochastic sir model with vertical transmission and vaccination. *Chaos, Solitons & Fractals*, 139:110027, 2020.

[42] O. Sharomi and T. Malik. Optimal control in epidemiology. *Annals of Operations Research*, 251(1–2):55–71, 2017.

[43] Z. Feng, S. Towers, and Y. Yang. Modeling the effects of vaccination and treatment on pandemic influenza. *Mathematical Biosciences*, 234(1):1–9, 2011.